For all alloys, the lithium contents varies between 1.7 and 2.9 wt%. Densities range from about 2.52 to 2.58 g/cm^3. Compared to conventional high-strength aluminium alloys such as 2024 (2.77 g/cm^3) or 7475 (2.80 g/cm^3), this represents a decrease in density of about 7–10%.

Of all the alloys listed in Table 1, only four have been registered to date by the Aluminum Association: 2090, 2091, 8090, and 8091. It is obvious from Table 1 that only Alcan has registered all of its alloys so far, whereas both Alcoa and Pechiney still have some alloys at an early development stage. Of the four alloys internationally registered, the two 809X series alloys show some advantage in density over the two 209X variants.

To compare the different alloys of the three companies, it is necessary to categorize them. This has been done in Table 2 where the new Al-Li alloys are put into various alloy categories along with the conventional high-strength alloys to be replaced. It should be mentioned that the categorizing in Table 2 can only serve as a rough classification for various reasons. First, the table does not distinguish between product forms such as sheet, plate, extrusions, or forgings. Second, the category can very well change with product form. Third, the same alloys might be found in several categories because the table does not distinguish between different tempers. Finally, the classification of the various new Al-Li alloys is not definite since some alloys listed in Table 2 are still undergoing extensive development, e.g., X 8092, X 8192, or CP 277.

Most advanced, and at the edge of widespread commercial application, are the damage-tolerant Al-Li alloys followed by the medium-strength variants. These two categories would also allow the three producers to go for one common alloy: 8090. This RAE-patented alloy is jointly registered by Alcan and Pechiney and slightly modified by Alcoa (see Table 1).

Sticking to the least possible number of different alloys has been a major demand of the aircraft industry. For the three high-strength Al-Li alloys proposed, no such commoness has come in sight. Furthermore, these alloys still need to undergo extensive development, as does the category of very low density alloys. Due to their high strength and/or high lithium content, they often do not yet meet the ductility or toughness goals required to match the properties of the corresponding conventional Al alloys they intend to replace.

IV. Commercial Applications

Although new materials in aerospace are usually first tested on military aircraft, their use in civil aircraft is considered to be more important since this can demonstrate two things at a time: First, the confidence in the new material attesting it a sufficient degree of maturity and, second, the economical superiority over the present solution. In the case of Al-Li alloys, this means that their use in military airplanes demonstrates that Al-Li alloys *can* fly, whereas use in civil aircraft shows that they can fly *economically*.

The Boeing Commercial Airplane Company announced the first use of an Al-Li alloy on a commercial airplane. The Alcoa alloy 2090 was chosen as the material for tow fittings on four B-747 front landing gear struts (see Fig. 2). These fittings are the attachment point for the tractors that are used to tow 747s at airports. They experience high loads during towing and are extensively exposed to the elements during all takeoffs and landings. The fittings are 7% lighter than the standard alloy fittings they replace.

The next major step was made by the McDonnell Douglas Aircraft Company. It decided to use 2090 extrusions for floor beams on its first five MD-11 transports to be delivered in 1990. Here, Al-Li parts are expected to reduce the aircraft weight by about 145 kg. About 55% of the weight savings are attributed to the reduced density of the alloy, and the rest is a result of the improved mechanical properties.

Airbus Industrie has announced that the new A330/A340 may see the introduction of Al-Li alloys. This will probably not be the case initially, but Al-Li alloys may well be introduced at a certain point in the production run. In a first step, stringers and parts of the secondary structure will be made out of Al-Li alloys. Then use of Al-Li sheet material for the fuselage skin will be attempted.

V. Outlook

As it looks today, damage-tolerant and medium-strength Al-Li alloys are at the edge of becoming commercial construction material. Further research and development work still has to be performed on the very high-strength and/or low-density alloys especially to meet the ductility and toughness goals. Grain boundary embrittlement needs to be fully understood as well as the various forms of anisotropy so that measures can be taken to eliminate these undesired properties.

More insight is necessary to better understand the corrosion properties, general corrosion as well as stress corrosion cracking. A consensus has to be found on what are the appropriate short-term corrosion tests. For this reason, more data need to be generated on long-term outdoor field tests.

Quite surprisingly, there is a problem of capacity. The question has been raised whether the aluminium companies can produce enough Al-Li to meet the quantity and schedule requirements of aerospace programs. This is, however, considered to be a short-term problem, which should be overcome once demand is manifested by extended orders for series aircraft. A prerequisite for the extended use of Al-Li alloys is, however, a solution to the scrap problem.

The future is already directed toward second- and third-generation Al-Li alloys, which includes material processed via the powder metallurgy route. Furthermore, Al-Li alloys can also be quite attractive candidates for metal matrix composites or for hybrid composite laminates like ARALL.

Takeoff Characteristics of Turbofan Engines

Young B. Suh*
Texas A&M University, College Station, Texas 77843

Nomenclature

AR = aspect ratio, $=(2s)^2/A_s$
A,B,C = constants in Eqs. (6) and (8)
A_s = span area
C_D = drag equation, $=C_{D0}+\phi KC_L^2$
D = drag
D_A = aerodynamic drag
e = Oswald's wing efficiency
f = fuel-air ratio
g = gravitational acceleration
h = span height above ground
K = $(\pi ARe)^{-1}$
L = lift
L_r = lapse rate of troposphere
$\dot{m}_{C,H}$ = air-flow rate (cold/hot), $\dot{m}_C=\beta\dot{m}_H$
$\dot{m}_{\text{in}}$ = intake air-flow rate, $=\dot{m}_C+\dot{m}_H$
S_{TO} = takeoff ground-rolling distance
s = half-span

Received Jan. 14, 1989; revision received Oct. 27, 1989.

*Mechanical Engineering Department. Member AIAA.

Table 1 Aerodynamic parameters of some aircraft

Aircraft (powerplant)[a]	s, m	A, m^2	AR	h, m	e[b]	K	ϕ (Suh-Ostowari)
B727-200 (3 TF)	16.46	157.9	6.86	2.32	0.85	0.053	0.403
B747-200 (4 TF)	29.82	511.0	6.96	6.46	0.85	0.053	0.544
MD-DC-10 (3 TF)	20.21	364.3	4.48	4.42	0.85	0.092	0.547
C-5A (4 TF), Galaxy	33.94	576.0	8.00	5.60	0.85	0.092	0.455
C-130 (4 TP), Hercules	20.21	162.12	10.1	4.97	0.85	0.037	0.584
C-141B (4 TF), Starlifter	24.37	299.88	7.92	3.26	0.85	0.047	0.385
B-1B (4 TF)[b]	20.85	181.2	9.6	3.24	0.80	0.0414	0.468
F-4C (2 TJ), Phantom	5.85	49.24	2.82	2.09	0.7	0.161	0.750
F-14A (2 TF), Tomcat[b]	9.77	52.49	7.27	2.37	0.7	0.063	0.654
F-15C (2 TF), Eagle	6.53	56.5	3.02	2.22	0.7	0.151	0.738
F-16 (1 TF), Fighting Falcon	5.00	27.87	3.59	1.92	0.7	0.127	0.767
F-18 (2 TF), Hornet	6.20	37.16	4.13	1.62	0.7	0.110	0.673

[a]TF = turbofan, TJ = turbojet, TP = turboprop. [b]Here wing efficiency e was assumed.

T = thrust
T_{sea} = absolute temperature of ISA at sea level
T_{static} = static thrust
U = aircraft speed
U_C, U_H = exhaust speeds of cold/hot jets
V_{TO} = takeoff speed
V_S = stall speed
W = weight of aircraft
z = altitude
β = bypass ratio
γ = ratio of specific heats (cold)
γ_H = ratio of specific heats (hot)
η_b, η_n = burner and nozzle efficiencies
μ = coefficient of rolling friction
ρ = density of air
σ = relative density
ϕ = drag reduction factor

Introduction

IT is desirable to have reliable working formulae for the takeoff characteristics of aircraft with turbofan engines. These should include the ground-rolling distance, fuel consumption, and rolling time, etc.

It is our purpose to derive these expressions for turbofan engines with bypass ratio β. The analysis of the takeoff performance of aircraft should incorporate a proper ground effect. There exist several expressions for the drag reduction factor ϕ in the drag equation. Here we use the form recently obtained by Suh and Ostowari,[1] which reads

$$C_D = C_{C0} + \phi K C_L^2, \quad K = (\pi A R e)^{-1}, \quad AR = (2s)^2/A_s$$

$$\phi = 1 - \frac{2e}{\pi^2}\ell n\left[1 + \left(\frac{\pi s}{4h}\right)^2\right] \tag{1}$$

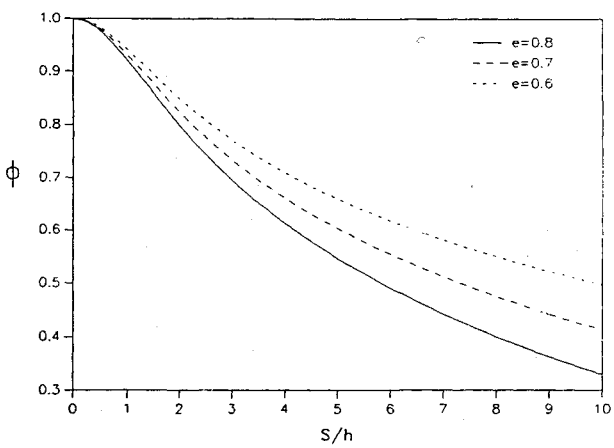

Fig. 1 Drag reduction factor.[1]

The drag reduction factor ϕ is reproduced in Fig. 1. Here C_{D0} includes the drags due to landing gears and flaps as well as parasite drag of wing-fuselage combinations. Table 1 lists ϕ together with other aerodynamic parameters for various classes of aircraft. The assumed Oswald's wing efficiency e is explicitly indicated. The takeoff ground-rolling distance (S_{TO}) up to nose-up configuration is given as

$$S_{TO} = \int_0^{V_{TO}} \frac{U\,dU}{T - D}$$

$$T - D = T - D_A - \mu(W - L)$$

$$W = Mg, \qquad D_A = \frac{1}{2}\rho U^2 A_s C_D$$

$$L = \frac{1}{2}\rho U^2 A_s C_L, \quad V_{TO} \simeq 1.2 V_S, \quad V_s = \left[\frac{2W}{\rho A_s C_L(\max)}\right]^{1/2} \tag{2}$$

The thrust of a turbofan engine is given by[2]

$$T(U) = \dot{m}_{in}\left[U_H(1+f) - U + \beta(U_C - U)\right]/(1+\beta) \tag{3}$$

In Eq. (3), it was assumed that both cold and hot jets at nozzle expand to the ambient pressure, which is a good approximation at low subsonic jet speeds (see Fig. 2). Notice that the so-called static thrust $T_{static} = T(0)$ is higher than the above $T(U)$ by $\dot{m}_{in}U$, namely $T_{static} = T(U) + \dot{m}_{in}U$. Figure 3 illustrates the variation of T_{static} with β. The parameters used are listed in Table 2.

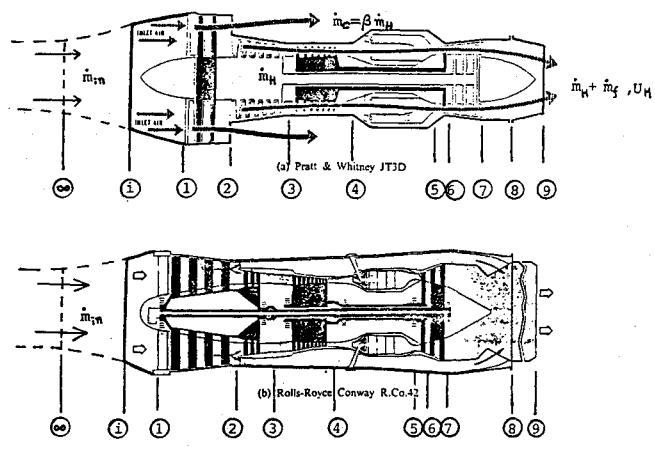

Fig. 2 Schematics of conventional turbofan engines. There could be an afterburner between station 7 and 8 (for example, Pratt-Whitney F100).

Table 2 Parameters used in Figs. 3–8

$f = 0.02$, $h = 2.18$ m, $A_s = 55$ m^2, $s = 6.5$ m, $\eta_n = 0.95$, $e = 0.7$
μ (dry, unbraked) = 0.02, $\rho = 1.225$ kg/m^3, P_∞[a] = 14.7 psi, $\dot{m}_{in} = 100$ kg/s
$R = 287$ J/kg K, $\gamma = 1.4$, $\gamma_H = 1.32$, $AR = 3.073$, $K = 0.148$
$C_D = 0.014 + \phi K C_L^2$ (drag equation), C_L(max) = 2.5, C_L (takeoff) = 0.93
T_{08}[a] = 745 K, $P_{08} = 21$ psi, $T_{02} = 327$ K, $P_{02} = 21.8$ psi

[a]T,P data from Pratt-Whitney, JT9D-7R4A Turbofan.

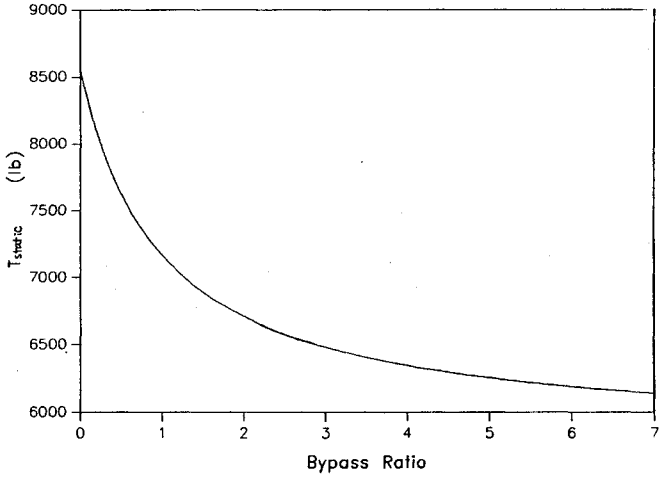

Fig. 3 Effect of the bypass ratio on the static thrust of turbofan engine.

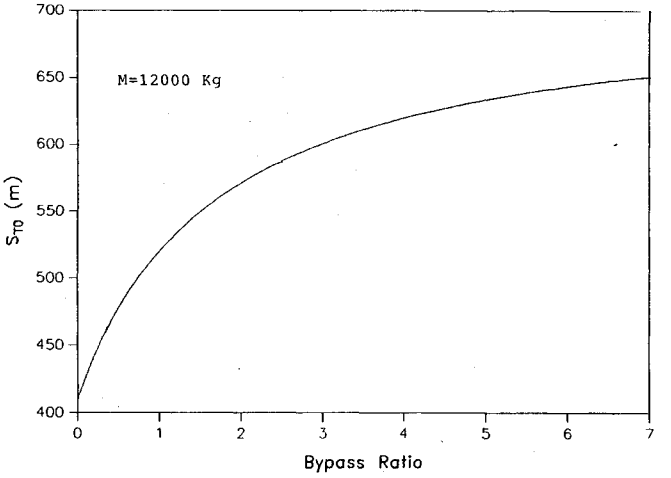

Fig. 4 Effect of bypass ratio on the takeoff ground roll.

For completeness, we here give the explicit formulae for U_H and U_C in terms of the internal thermodynamic parameters of the engine[2];

$$U_H = \sqrt{\left[\frac{2\gamma_H}{(\gamma_H - 1)}\right] RT_{08}\eta_n \left[1 - \left(\frac{P_\infty}{P_{08}}\right)^{\frac{\gamma_H - 1}{\gamma_H}}\right]}$$

$$U_C = \sqrt{\left[\frac{2\gamma}{(\gamma - 1)}\right] RT_{02}\eta_n \left[1 - \left(\frac{P_\infty}{P_{02}}\right)^{\frac{\gamma - 1}{\gamma}}\right]} \qquad (4)$$

where η_n is the adiabatic nozzle efficiency and 0 refers to the stagnation state. The ratio of specific heats are $\gamma = 1.4$ and $\gamma_H \simeq 1.32$, and the other thermodynamic parameters can be found from the engine manufacturer's brochure. The fuel-air ratio f is relatively independent of the flight speed and primarily depends on the temperature limit imposed by the turbine blade material. This is also given as

$$f = \frac{(T_{05}/T_{04}) - 1}{(\eta_b Q_R / C_P T_{04}) - (T_{05}/T_{04})} \qquad (5)$$

where η_b is the burner efficiency and Q_R the heating value of the hydrocarbon used as an aviation fuel (Btu/lbm). This ratio is much smaller than the stoichiometric ratio. Typical range of f is $0.01 \sim 0.02$ for usual annular-can type combustors. Later in our discussion, we will show that all the takeoff characteristics may well be expressed in terms of the static thrust T_{static}, which is always readily available for the given engines.

Takeoff Ground Roll and Fuel Consumption

Equation (2) for the takeoff ground roll can be integrated exactly and yields

$$S_{TO} = \frac{-M}{2A} \ell n \left[1 - \frac{V_{TO}}{C}(AV_{TO} + B)\right] - \frac{MB}{A\sqrt{B^2 + 4AC}} \times \left(\tanh^{-1}\frac{2AV_{TO} + B}{\sqrt{B^2 + 4AC}} - \tanh^{-1}\frac{B}{\sqrt{B^2 + 4AC}}\right) \qquad (6)$$

where

$$A = \frac{1}{2}\rho A_s (C_D - \mu C_L)$$

$$B = \dot{m}_{in}$$

$$C = \frac{\dot{m}_{in}}{1 + \beta}\left[U_H(1 + f) + \beta U_C\right] - \mu W = T_{static} - \mu W$$

The constant A depends on the aerodynamic parameters, whereas C depends on the engine characteristics and weight of the aircraft. S_{TO} is shown plotted in Figs. 4 and 5. The constants used for these plots are listed in Table 2.[3,4]

In order to derive the fuel consumption during takeoff ground roll, we first note that the fuel flow rate is given by

$$\dot{m}_f = f\dot{m}_H = f\dot{m}_{in}/(1 + \beta) \qquad (7)$$

Accordingly, the total fuel consumption (up to nose-up) will be

$$M_f = \int_0^{t_{TO}} \dot{m}_f \, dt = \dot{m}_f \int_0^{V_{TO}} \frac{M \, dU}{T - D}$$

This is integrated and gives

$$M_f = \frac{2Mf\dot{m}_{in}}{(1 + \beta)\sqrt{B^2 + 4AC}} \times \left(\tanh^{-1}\frac{\dot{m}_{in} + 2AV_{TO}}{\sqrt{B^2 + 4AC}} - \tanh^{-1}\frac{\dot{m}_{in}}{\sqrt{B^2 + 4AC}}\right) \qquad (8)$$

where A, B, and C are the same as those given in Eq. (6). These are seen plotted in Figs. 6 and 7 for the same case listed in Table 2.

Finally, the rolling time up to nose-up configuration will be

$$\Delta t_{roll} = M_f/\dot{m}_f = M_f(1 + \beta)/(f\dot{m}_{in}) \qquad (9)$$

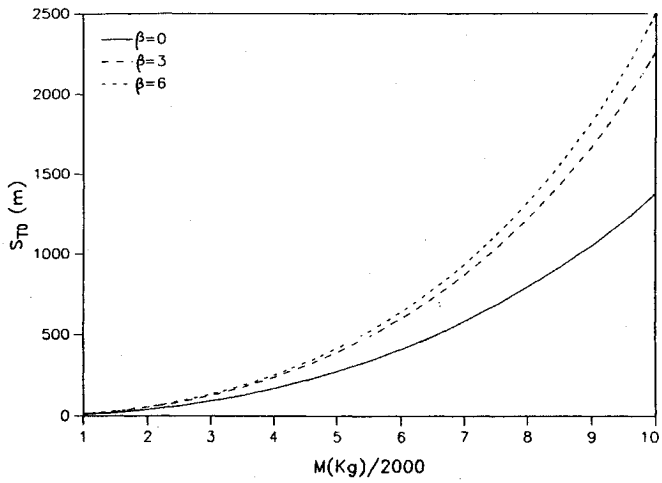

Fig. 5 Effect of aircraft weight on the takeoff ground roll.

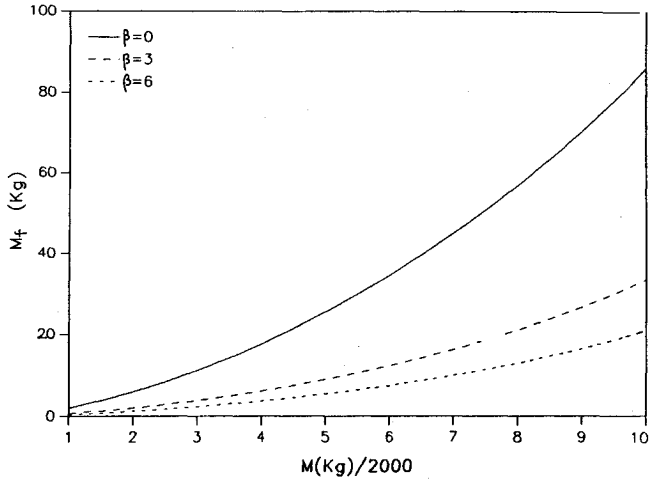

Fig. 7 Effect of aircraft weight on the takeoff fuel consumption.

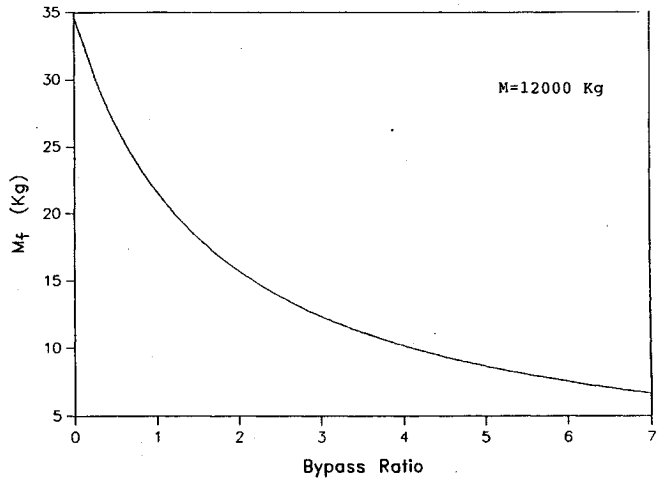

Fig. 6 Effect of bypass ratio on the fuel consumption at takeoff.

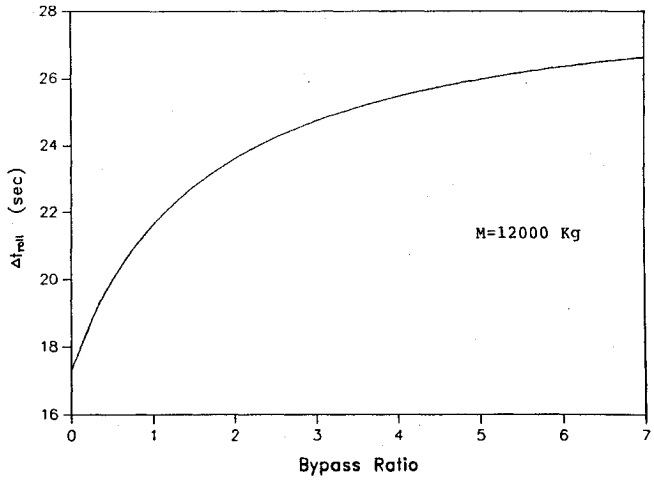

Fig. 8 Effect of bypass ratio on the takeoff rolling time up to nose up.

where M_f is given by Eq. (8). Figure 8 illustrates this rolling time.

Furthermore, the comparison of Eq. (6) with (8) yields S_{TO} in terms of M_f as

$$S_{TO} = \left[\rho A_s(\mu C_L - C_D)\right]^{-1}\left\{M \ell n\left[1 - \frac{V_{TO}(AV_{TO} + \dot{m}_{in})}{T_{static} - \mu W}\right] + M_f(1+\beta)/f\right\} \quad (10)$$

Consequently, by knowing the fuel consumption during ground roll, one can obtain the rolling distance and time taken before the nose-up configuration through Eqs. (10) and (9), where M_f was given in Eq. (8).

Results and Discussion

As are shown in the preceding figures, the bypass ratio has substantial effects on the takeoff performances of an aircraft with turbofan engines. Notice that the turbofan of $\beta = 0$ reduces to turbojet engine. However, Fig. 5 shows that the bypass ratio has little influence on the takeoff ground-rolling distance if $\beta \geq 3$. The reason is that greater cold air flow rate ($\dot{m}_C = \beta \dot{m}_H$) favorably contributes to the thrust despite the fact that the speed of the cold jet is not comparable with that of the hot exhaust jet. Although the present analysis did not begin with the case when the afterburner is turned on, all the formulations given are equally valid for this thrust augmentation as far as T_{static} is available. Furthermore, if T_{static} is given at the sea level, as is the usual case by the engine manufacturers, the correct value of T_{static} appropriate to the airfield under consideration can be found easily using the property of International Standard Atmosphere (ISA) troposphere, namely $T_{static}(z) = \sigma T_{static}$(sea level), where σ is the relative density and z is the altitude.

It is not hard to show that

$$\sigma(z) = \left(1 - \frac{zL_r}{T_{sea}}\right)^{(g - RL_r)/RL_r} = (1 - 2.256 \times 10^{-5} \cdot z)^{4.256} \quad (11)$$

where $g = 9.81$ m/s^2, $L_r = 0.0065°$ k/m, $T_{sea} = 288.16$ K. For the multiple engines $\dot{m}_{in}$ is to be replaced by $n\dot{m}_{in}$, n being the number of identical engines.

Finally, it should be understood that Eq. (6) gives the rolling distance up to the rotation (nose-up) configuration, not the takeoff distance defined by Federal Aviation Regulations (FAR), i.e., whole horizontal distance covered up to the screen height of 35 ft above the ground.

References

[1]Suh, Y. B., and Ostowari, C., "Drag Reduction Factor Due To Ground Effect," *Journal of Aircraft*, Vol. 25, No. 11, 1988, pp. 1071-1072.

[2]Hill, P. G., and Peterson, C. R., *Mechanics and Thermodynamics of Propulsion*, Addison-Wesley, Reading, MA, 1965.

[3]Bathie, W. W., *Fundamentals of Gas Turbines*, Wiley, New York, 1984.

[4]Treager, I. E., *Aircraft Gas Turbine Engine Technology*, 2nd ed., McGraw-Hill, New York, 1979.